INŽENÝRSKÁ MECHANIKA 2005
NÁRODNÍ KONFERENCE
s mezinárodní účastí
Svratka, Česká Republika, 9. -12. května 2005

BUCKLING AND POSTBUCKLING BEHAVIOUR OF LAMINATE PLATES WITH EMBEDDED CIRCULAR-SHAPED DELAMINATIONS

V. Obdržálek[*†], **J. Vrbka**[*]

Summary: *A finite-element model has been developed to study buckling and post-buckling behaviour of a square plate made of fibre-metal laminate with one or two delaminations. A study into the effect of orientation of composite plies and through-the-thickness position of delaminations upon the buckling load and load-bearing capability of buckled plates was performed. The results indicate significant reduction of buckling loads for plates with near-surface delamination and certain ply angles.*

1 Introduction

Laminate components are susceptible to a number of failure modes. Delamination – loss of connectivity between adjacent plies – is one of the most common. It can have two fold impact on the load-bearing capability of laminate structures. Firstly, delamination leads to lower stiffness of a laminate part in comparison to a non-delaminated one and consequently this leads to lower buckling loads. Secondly, local buckling of a delaminated sublaminate leads to a non-uniform stress field in the part and results in its pronounced damage.

In the last fifteen years the problem of delamination buckling has been intensively studied. Various approaches has been adopted to predict the behaviour of delaminated plates subjected to compressive or shear loading, both of which could cause buckling of the plate. Most researchers have focused on simplified problems such as 1D beam-plate models or plates with through-the-width delaminations. Although this provide us with deeper insight into the problematics, their approach has a limited application when safety of a real structure is to be predicted. Only a few works on buckling of plates with multiple embedded delaminations were published recently.

Kim and Kedward (1999) used Rayleigh-Ritz method to predict global and local buckling loads of a plate with a single delamination. Their approach for predicting global buckling behaviour can also be extended for multiple delaminations. Kouchakzadeh and Sekine (2000) did linear buckling analysis of plates with multiple eliptic delaminations. Overlapping of sublaminates was prevented by penalty functions. Hwang and Liu (2001) performed nonlinear analysis

[*]Institute of Solid Mechanics, Mechatronics and Biomechanics, Faculty of Mechanical Engineering, Technical University Brno, Technická 2, Brno 616 69, Czech Republic
[†]*Email address:* obdrzalek@fme.vutbr.cz

of 2D model of a plate with multiple delaminations. Wang and et al. (2005) compared experimental mesurements and finite element predictions of out-of-plane displacements of composite plate with two square delaminations. Kyuong et al. (1999) conducted comprehensive study on buckling and postbuckling of plates with multiple through-the-width and embedded delaminations using structural shell elements. Overlapping of sublaminates in the debonded region was prevented by virtual beam elements.

This paper presents results of an investigation into the effect of through-the-thickness position of one and two circular delaminations upon the buckling and postbuckling behaviour of a square fibre-metal laminate plate. Non-linear finite element analysis was performed using finite-element system ABAQUS v 6.4.

2 Analysis description

Behaviour of a square uniaxially compressed plate (see Figure 1) with simply supported edges was studied. The compressive load was applied to the plate by uniform displacing of two opposite edges. Location of delaminations and the ply angle of the composite laminae were varied to obtain information about the optimum laminate structure. The plate was made of

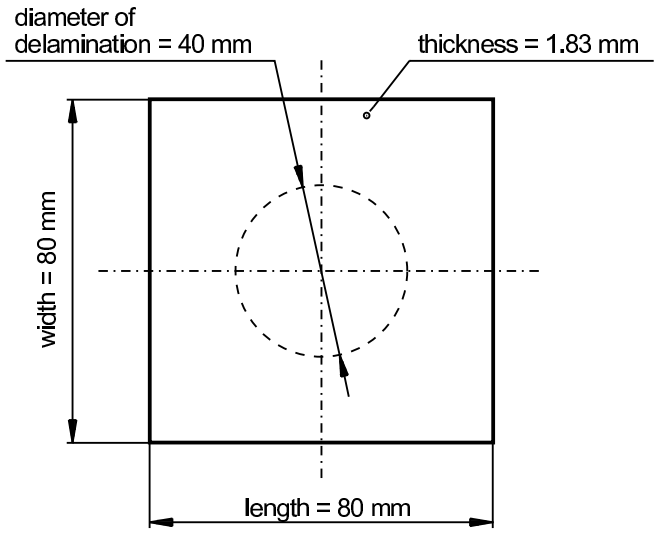

Figure 1: Dimensions of the plate.

fibre-metal laminate, which consisted of three aluminium alloy layers interlieved with long-fibre composite plies. Stacking sequence and thicknesses of individual plies are summarised in Table 1, material properties are listed in Tables 2 and 3. The plate contained either one or two embedded circular delaminations, which could be located only at the interfaces between plies. In the following sections the interfaces at which delaminations were positioned are entitled with letters as listed in the last column in Table 1.

3 Finite element model

A semi-parametric finite element model of the plate was built using eight-node continuum shell element (SC8R). The number of elements through the thickness of the plate was equal the num-

Table 1: Structure of the laminate. Orientation of composite plies is given with respect to the loading direction.

Layer	thickness [mm]	orientation	interface
aluminium	0.4	—	A
composite	0.1575	$+\theta$	B
composite	0.1575	$-\theta$	C
aluminium	0.4	—	D
composite	0.1575	$-\theta$	E
composite	0.1575	$+\theta$	F
aluminium	0.4	—	

Table 2: Material properties of composite plies.

Hexcel unidirectional carbon/epoxy prepreg		
$E_{11} = 126.0$ GPa	$E_{22} = 11.0$ GPa	$E_{33} = 11.0$ GPa
$\nu_{12} = 0.28$	$\nu_{13} = 0.28$	$\nu_{23} = 0.40$
$G_{12} = 6.60$ GPa	$G_{13} = 6.60$ GPa	$E_{23} = 3.93$ GPa

ber of delaminations plus one. Elements were refined along the boundary of the delaminated area in order to achieve higher accuracy. A typical finite element mesh is shown in Figure 2.

Delaminations were modelled only between two adjacent laminae. An initial imperfection was formed by inclusion of a virtual interference between plies at the delaminated region. In the case of a plate with two delaminations, such a condition was prescribed at the delaminated region which was closer to the surface of the plate. The interference magnitude was chosen to be 1.10^{-5} m. Contact conditions were employed to prevent inadmissible interpenetration of elements in the delaminated region.

Some arrangements were made to simulate simply supported boundary conditions. Nodes on the boundary of the plate were constrained to lie on a straight line defined by nodes with the same in-plane coordinates (Multi-Point Constraint type SLIDER). Moreover, a set of linear equations was employed to connect nodes on the top and bottom surfaces with an extra set of nodes (zero nodes in Figure 3) positioned along the boundary of the plate on its mid-surface.

Table 3: Material properties of metal plies. True plastic strains ε_{pi} and corresponding Cauychy stressses σ_{yi} are used to define behaviour of the material in the elasto-plastic region.

2024 T6 aluminium alloy	
$E = 0.725$ GPa	$\nu = 0.34$
$\sigma_{y1} = 360$ MPa	$\varepsilon_{p1} = 0.000$
$\sigma_{y2} = 521$ MPa	$\varepsilon_{p2} = 0.077$

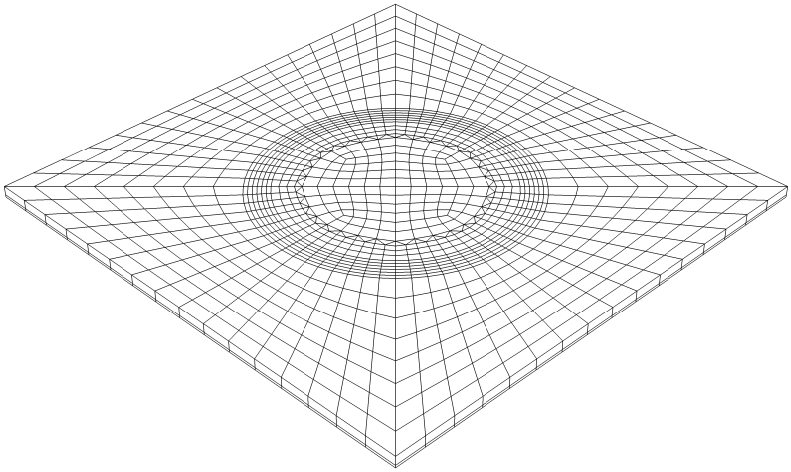

Figure 2: Finite element mesh

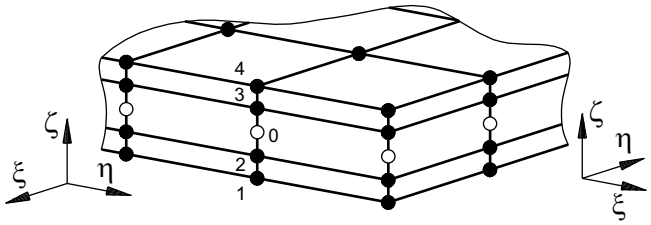

Figure 3: Application of constraints on nodes lying on the plate's boundary. Nodes 0-4 are constrained to lie on a straight line and their dispacements are interconnected through a set of linear equations (1). Zero nodes form an extra set of nodes with no connectivity to elements.

These equations take the form of

$$\begin{aligned} u_\xi^a + u_\xi^b - 2u_\xi^0 = 0 \\ u_\zeta^a + u_\zeta^b - 2u_\zeta^0 = 0 \\ u_\eta^a + u_\eta^b - 2u_\eta^0 = 0 \end{aligned} \tag{1}$$

where u_i^a, u_i^b and u_i^0 are displacements in the i-direction of the nodes on the top, bottom and middle surface respectively. Only to these extra nodes were then the appropriate displacements prescribed. In concrete terms, zero out-of-plane displacement along all edges of the plate, uniform compressive in-plane displacement along two opposite edges and finally in-plane displacement perpendicular to the loading direction was set zero at one corner node.

The Newton-Raphson solution technique with stabilization algorithm was used to overcome divergence problems which are interrelated with stability problems and therefore the postbuckling behaviour could have been studied.

4 Results

Results are presented for the non-delaminated plate and all unique variants of the plate with one or two delaminations. For each of these, ten analysis runs for ten different ply angles were

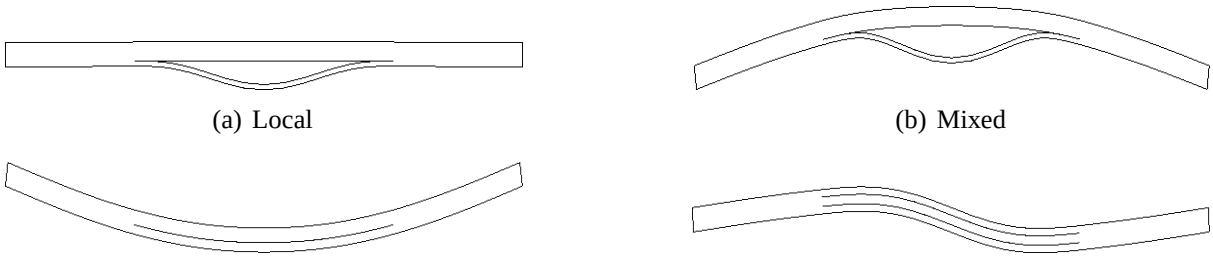

(a) Local (b) Mixed

(c) Global - U shape (d) Global - S shape

Figure 4: Buckling mode shapes

carried out. The angle was varied from 0° to 90° with 10° increment. In the following sections the initial buckling loads, buckling mode shapes and load-bearing capability of the plates is discussed.

4.1 Buckling modes

Summary of the buckling modes is given in Table 4 and examples of the respective load - out-of-plane displacement curves are presented in Figure 5. It can be seen, that we can distinguish three groups of plates.

The first group comprises of plates that exhibited mixed buckling mode. Most of these have a delamination in the topmost position, which means that the near-surface sublaminate is thin and has a lower stiffness in comparison with the other sublaminate and can therefore start to buckle locally (Figure 4(a)). Two exceptions are found here - the plate with a single delamination at the B interface and the plate with delaminations at the B and C interfaces. For both of these the above conclusion remains true as the thicker sublaminate is still considerably stiffer than the remaining thinner sublaminates. It should also be noted, that for some plates a snap-like change from the initially flat geometry to the buckled one was observed as it can be seen in Figure 5(a). Because this behaviour sometimes occured together with the negative pivot problem during the analysis, an extra dynamic explicit analysis was carried out to confirm these findings. Although the analysis was not quasi-static - some vibrations were present, a similar trend was observed and so it is possible that this behaviour may be realistic. Moreover, a similar result was obtained experimantally by Short et al. (2001), who studied postbuckling behaviour of a square plate with a square delamination. They explained this behaviour by the residual adhesion between sublaminates.

In the second and third group we can found plates that exibited global buckling mode. The plates in the second group buckled into the U shape and plates in the third group into the S shape - see Figure 4. It should be noted, that only the plates with two delaminations are found in the third group. Focusing now on the load-deflection curves (Figure 5) of the plates with two delaminations we can see, that for the plates with the topmost delamination located at the B interface, some gap between sublaminates was always present after initial buckling and all the sublaminates buckle in the same direction. For the plates with small angle ply this gap closed as the load increased and the global buckling mode shape was established. On the other hand, the plates with the topmost delamination located at the A interface exhibited the mixed buckling mode after inital buckling, and only after load increase their geometry changed to that of S shape. Such a complicated behaviour can not be easily explained, but extension-

Table 4: Buckling modes summary. M - mixed, GU - global U-shaped, GS - global S-shaped;
Indices: S - snap-like initiation of buckling, 1 - initial buckling mode was global U shaped with gap between sublaminates, 2 - initial buckling mode was mixed. See Figures 4 and 5.

Delaminated	Ply angles									
interface(s)	0	10	20	30	40	50	60	70	80	90
None	GU	GU	GU	GU	GU	GU	GU	GU	GU	GU
A	M	M	M	M	M	M	M	M	M	M
B	GU_1	GU_1	GU_1	M	M	M	M	M	M	M
C	GU	GU	GU	GU	GU	GU	GU	GU	GU	GU
A&B	M_S	M_S	M_S	M_S	M_S	M_S	M	M	M	M
A&C	M_S	M_S	M_S	M_S	M_S	M_S	M	M	M	M
A&D	M	M	M	M	M	M	GS_2	GS_2	GS_2	GS_2
A&E	M	M	M	M	M	GS_2	GS_2	GS_2	GS_2	GS_2
A&F	M	M	M	M	M	M	GS_2	GS_2	GS_2	GS_2
B&C	M_S	M_S	M_S	M_S	M_S	M_S	M	M	M	M
B&D	GU_1	GU_1	GU_1	GS_1	GS_1	GS_1	GS_1	GS_1	GS_1	GS_1
B&E	GU_1	GU_1	GU_1	GS_1	GS_1	GS_1	GS_1	GS_1	GS_1	GS_1
C&D	GU	GU	GU	GS_1	GS_1	GS_1	GS_1	GS_1	GS_1	GS_1

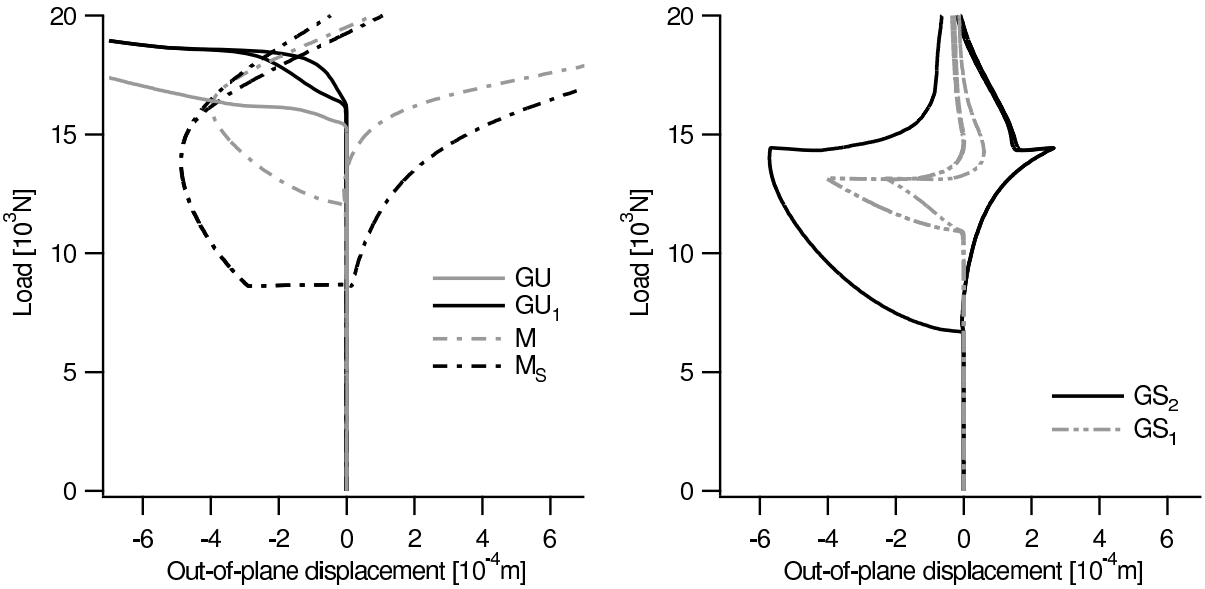

(a) Mixed and global U-shaped buckling modes.

(b) Global S-shaped buckling modes.

Figure 5: Typical load – out-of-plane displacement curves in the in-plane centre of the plate.

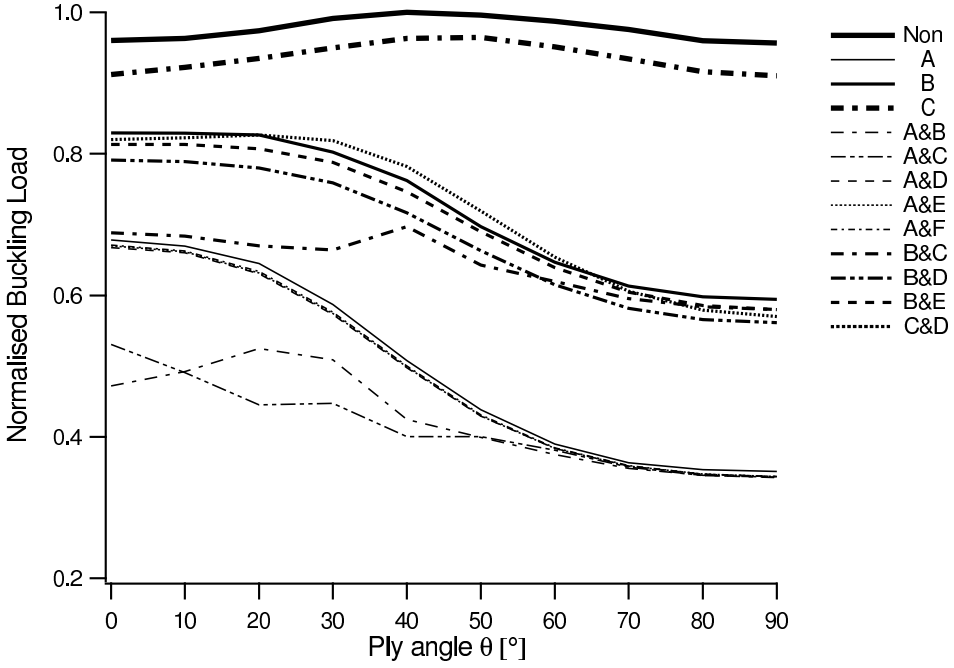

Figure 6: Normalised buckling loads vs. ply angle θ

bending and bending-twisting coupling effects due to the unsymmetric stacking sequence of the sublaminates together with the global plate stiffness are expected to be the possible cause.

4.2 Buckling loads

In Figure 6 normalised initial buckling loads are plotted versus ply angle of the composite laminae. The buckling loads were normalised with respect to the maximum buckling load of the non-delaminated plate $F_{norm} \doteq 19415N$. This load and the corresponding ply angle $\theta \doteq 41^\circ$ were found by differentiation of the polynomial fitting function of the buckling load values for this plate. It can be seen that the closer to the surface was the delamination the lower was the buckling load. Focusing on the plates with two delaminations, it can be concluded, that the existence of the second delamination caused further reduction of the buckling load. This effect was more considerable for close delaminations.

4.3 Load-bearing capability

It is well known that the failure process of laminates is quite complicated and usually more than one failure mechanism can be observed. In this paper only the initiation of plastic deformation of metal plies is considered because developement of plastic deformation provides some information about stress concentrations in the plate, appropriate material characterictics were available and because it is probable, that the yielding of metal layers would precede growth of the delaminations. Therefore the moment at the onset of plastic deformation was used to determine the limit load. In Figure 7 normalised limit loads are plotted versus ply angle of the composite laminae. The limit loads were normalised with respect to the maximum limit load of the non-delaminated plate $F_{norm} \doteq 24617N$. Again as for the buckling loads it can be seen, that in the case of a plate with near-surface delaminations, lower limit load was observed than

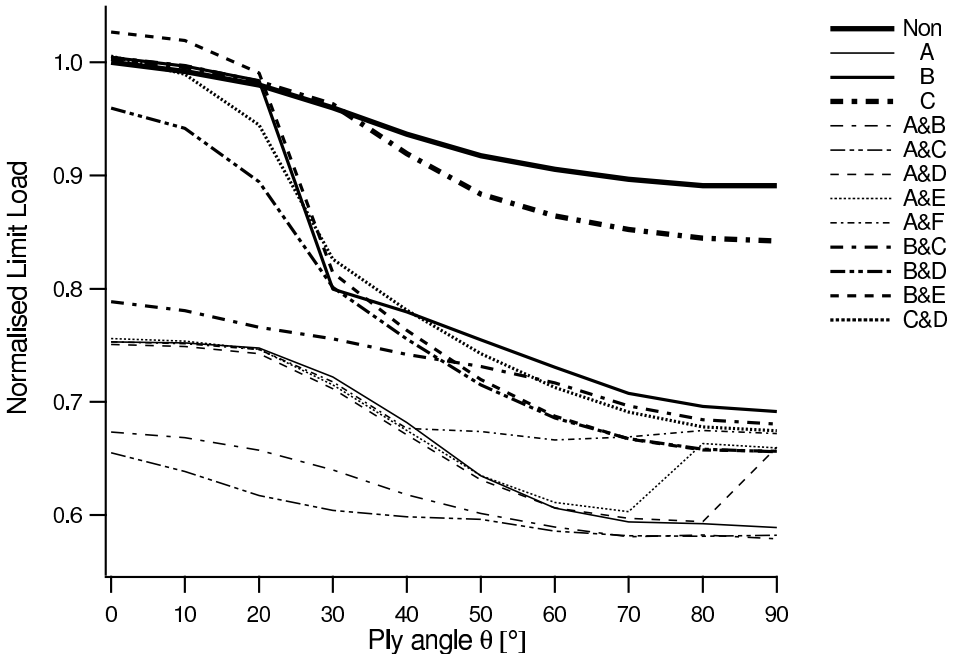

Figure 7: Normalised limit loads vs. ply angle θ

in case of a plate with delaminations near to the datum surface of the plate. Sudden changes in the limit loads for some variants of plates can be explained by change of the buckling mode from the mixed to the global one or by change from the local buckling to the global buckling mode before plastic deformation could have developed.

5 Conclusions

A non-linear finite element analysis of fibre-metal laminate plates with one or two circular delaminations was performed. A semi-parametric finite-element model was built using 8-node continuum shell element. Overlapping of sublaminates in delaminated region was prevented by contact algorithm. Through-the-thickness position of delaminations and orientation of composite plies were varied in order to find the optimum design.

Based on the numerical results, we can conclude:

- Delamination can significantly reduce both the buckling loads and limit loads of laminate plates.
- This reduction is more significant for plates with a near-surface delamination, for which cases the local buckling mode occurs.
- Plates with two delaminations can exhibit even more drastic reduction of the buckling and limit loads, if both delaminations are near the surface of the plate.
- Contrary to the common opinion (Jones (1975)) simply supported symmetric angle-ply laminate plates with the ply angle $\theta = 45^\circ$ may not provide the highest buckling loads.

Acknowledgement

This work was supported by the grant of Ministry of Education CR MSM 262100001.

References

Hwang, S. F. and Liu, G. H. (2001), Buckling behavior of composite laminates with multiple delaminations under uniaxial compression, *Composite Structures* **53**, pp. 235–243.

Jones, R. M. (1975), *Mechanics of composite materials*, McGraw-Hill, New York.

Kim, H. and Kedward, T. (1999), A method for modeling the local and global buckling of delaminated composite plates, *Composite Structures* **44**, pp. 43–53.

Kouchakzadeh, M. A. and Sekine, H. (2000), Compressive buckling analysis of rectangular laminates containing multiple delaminations, *Composite Structures* **50**, pp. 249–255.

Kyuong, W. M., Kim, C. G. and Hong, C. S. (1999), Buckling and postbuckling behavior of composite cross-ply laminates with multiple delaminations, *Composite Structures* **43**, pp. 257–274.

Short, G. J., Guild, F. J. and Pavier, M. J. (2001), The effect of delamination geometry on the compressive failure of composite laminates, *Composite Science and Technology* **61**, pp. 2075–2086.

Wang, X. W. and et al. (2005), Compressive failure of composite laminates containing multiple delaminations, *Composite Science and Technology* **65**, pp. 191–200.